RSC Advances

PAPER

View Article Online
View Journal | View Issue

Cite this: *RSC Adv.*, 2026, **16**, 18984

Gauging lipid vulnerabilities in mRNA-LNPs under various environmental stressors through TIMS-TOF analysis

Michael Girgis, †*[ac] Amir Saed,†[b] Suman Alishetty,[a] Manuel Carrasco,[a] Dillon O'neill,[a] Nabilah Baby,[a] Gregory Petruncio,[bc] Caroline Hoemann,[a] Mathew Albano,[d] Xuejun Peng,[d] Beixi Wang,[d] Erica Forsberg,[d] Mohammad Nazim Rahil,[b] Amany Saleh[e] and Mikell Paige*[bc]

The long-term stability of mRNA lipid nanoparticles (LNPs) is governed by the chemical resilience of their constituent lipids, yet the specific degradation pathways triggered by real-world stressors remain poorly defined. Here, we systematically mapped lipid-specific vulnerabilities in mRNA-LNPs formulated with three clinically relevant ionizable lipids, DLin-MC3-DMA (MC3), SM-102, and ALC-0315, under controlled thermal, photo-oxidative, and mechanical stress conditions. Luciferase-encoding mRNA-LNPs were prepared *via* microfluidic mixing using a standardized composition of ionizable lipid, helper phospholipid, cholesterol, and PEG-lipid, and then exposed, for 72 hours, to mild heat (28 °C), ultraviolet (UV, 360 nm) irradiation, hydrogen peroxide-mediated oxidation, or repeated freeze–thaw cycling. Ultra-high-pressure liquid chromatography coupled with trapped ion mobility time-of-flight mass spectrometry (UHPLC-TIMS-TOF MS) enabled high-resolution, structure-specific profiling of intact lipids and degradation products. We show that UV and oxidative stress, but not modest heat or freeze–thaw cycling, induce pronounced and lipid-dependent chemical degradation, including headgroup oxidation, ester hydrolysis, and bond cleavage within MC3, SM-102, and ALC-0315, as well as the helper lipid 1,2-distearoyl-*sn*-glycero-3-phosphocholine (DSPC). These modifications occur at levels and sites consistent with impaired endosomal escape chemistry, despite preservation of particle size, encapsulation efficiency, and conventional biophysical readouts. By directly linking defined environmental stressors to discrete ionizable lipid oxidation pathways, this work provides a mechanistic framework for understanding hidden failure modes in mRNA LNP formulations and establishes UHPLC-TIMS-TOF MS as a powerful tool for predictive stability assessment and rational design of more robust, regulation-ready mRNA therapeutics.

Received 16th November 2025
Accepted 3rd March 2026

DOI: 10.1039/d5ra08835f

rsc.li/rsc-advances

Introduction

In the rapidly evolving landscape of biomedical research and therapeutics, mRNA-based lipid nanoparticles (LNPs) have emerged as an integral tool for modern medicine.[1–12] Beyond vaccines, mRNA-LNPs are being explored for a myriad of applications, ranging from cancer treatments to genetic disorders, marking a potentially new era in personalized and precision medicine.[13–22] However, the journey from the laboratory to the clinic is fraught with challenges, the chief one among them being the stability and resilience of these LNPs.[23–26] The efficacy of mRNA-LNPs hinges on their ability to maintain structural integrity and functionality under various physiological and environmental conditions.[23,27,28] This calls for a deeper understanding of how external stress factors, such as light exposure, temperature fluctuations, and oxidative stress can impact LNP stability and, consequently, their therapeutic efficacy.[29–31]

Comprehensive evaluation of mRNA-LNP stability and degradation is critical in therapeutic contexts, since the physicochemical integrity of LNPs directly governs mRNA protection, delivery efficiency, and downstream biological activity. Stable LNPs protect the mRNA from degradation until it reaches the target cells, ensuring the therapeutic action of the mRNA is achieved.[32–34] Safety is another crucial aspect of LNP stability.[35,36] Understanding how LNPs degrade and what by-products they produce is essential to assess their safety profile. Safe degradation products that the body can easily clear minimize potential side effects, making the LNPs more suitable for medical use.[37–40]

[a]*Department of Bioengineering, College of Engineering & Computing, George Mason University, Fairfax, VA, USA*
[b]*Department of Chemistry & Biochemistry, College of Science, George Mason University, Fairfax, VA, USA. E-mail: myassagi@gmu.edu; Tel: +1-571 214 3460*
[c]*Center for Molecular Engineering, George Mason University, Manassas, VA, USA*
[d]*Bruker Scientific, Billerica, Massachusetts, USA*
[e]*Northern Virginia Community College, Manassas, Virginia, USA*
† The authors contributed equally.

Additionally, stability of LNPs informs the development of controlled release mechanisms. By designing LNPs to degrade under specific conditions, we can create systems that release the mRNA payload at a controlled rate.[41,42] This can enhance the treatment's efficacy and potentially reduce the dosage frequency.[43,44] Several research studies highlighted the crucial role of ionizable lipids on mRNA-LNPs efficacy and stability.[45–48]

The formulation of LNPs also plays a critical role in determining their stability and performance, as the specific lipid composition, molar ratios, and assembly conditions govern nanoparticle structure, cargo protection, and resistance to environmental stress.[49,50] The stability and degradation properties are influenced by the composition of LNPs, including the types of lipids used.

Lipids play a central role in defining the stability, efficacy, and safety of LNPs used for mRNA delivery.[49,51] Ionizable lipids are the core functional component dictating the structural stability, delivery efficiency, and safety profile of mRNA-LNPs. Their acid-responsive charge behavior enables efficient mRNA encapsulation and endosomal escape, remaining neutral at physiological pH to minimize cytotoxicity, yet becoming protonated in acidic endosomes to promote membrane fusion and cytoplasmic release.[52,53] However, the chemical integrity of ionizable lipids is a major determinant of LNP stability; oxidative or hydrolytic degradation of these lipids can compromise particle uniformity, reduce transfection efficiency, and increase inflammatory potential.[54,55] The alkyl chain composition, linker chemistry, and headgroup pK_a of ionizable lipids collectively modulate lipid packing, RNA complexation, and metabolic clearance, making their rational design essential for balancing potency and safety. While other lipids such as cholesterol, phospholipids, and PEG-lipids provide structural support and colloidal stability, it is the ionizable lipid component that ultimately governs the LNP's biophysical resilience and biocompatibility during storage, transport, and *in vivo* delivery.[56] Research in this area helps in optimizing these formulations for improved performance, such as better stability in blood and efficient delivery to target cells.[57–61]

Furthermore, the stability of LNPs under various storage and transport conditions is vital for their practical application, particularly in regions with limited cold chain infrastructure. This aspect is critical for ensuring that the therapeutic quality of mRNA therapies is maintained from production to administration. Finally, regulatory approval processes demand a thorough understanding of the stability and degradation of LNPs.[57,59–62]

In this study, LNPs were formulated with ionizable lipids (MC3, SM-102, and ALC-0315) were formulated independently using Spark NanoAssemblr™ (Precision NanoSystems) with a standard formulation technique.[23,24,47] To assess the stability and degradation properties of LNPs, an equal amount of LNPs was subjected to various stress conditions for 72 hours. These conditions included thermal stress by heating at 28 °C, exposure to UV light at a wavelength of 360 nm, oxidative stress by mixing with hydrogen peroxide to achieve a final concentration of 100 mM, and mechanical stress through freeze–thaw cycles, alternating between −20 °C for 12 hours and 22 °C (ambient temperature) for 12 hours.

Following the exposure to these stress conditions, lipids were extracted from the LNPs using a chloroform and methanol mixture. The lipid extracts were analyzed using a Bruker TIMS-TOF Pro mass spectrometer, which was equipped with a Bruker Elute ultra-high-performance liquid chromatography (UHPLC) system and a VIP-HESI source. Both full scan mass spectrometry (MS) and tandem MS (MS/MS) utilizing Parallel Accumulation-Serial Fragmentation (PASEF) techniques were employed in both positive and negative ion modes to comprehensively profile the lipid components. The resulting data were processed and analyzed using Metaboscape 2023 and Data Analysis 6.0 software programs, providing insights into the stability and degradation behavior of the LNPs under the tested conditions. Fig. 1 illustrates the principal environmental stressors that compromise the structural integrity of mRNA LNP formulations, including thermal exposure, oxidative conditions, UV irradiation, and repeated freeze–thaw cycles. These stressors can trigger lipid oxidation, hydrolysis, and phase destabilization, leading to the disruption of the nanoparticle architecture, leakage or degradation of encapsulated mRNA, and altered physicochemical properties. The representative LNP composition comprises ionizable lipids, helper phospholipids, cholesterol, and PEG-lipids, which together stabilize and protect the therapeutic nucleic acid cargo. To systematically characterize the molecular consequences of these stress conditions, LNP samples were analyzed using UHPLC-TIMS-TOF MS, enabling high-resolution profiling of degradation products and lipid oxidation intermediates.

In this context, the objectives of our research are threefold: Firstly, to unravel the intricate mechanisms by which external

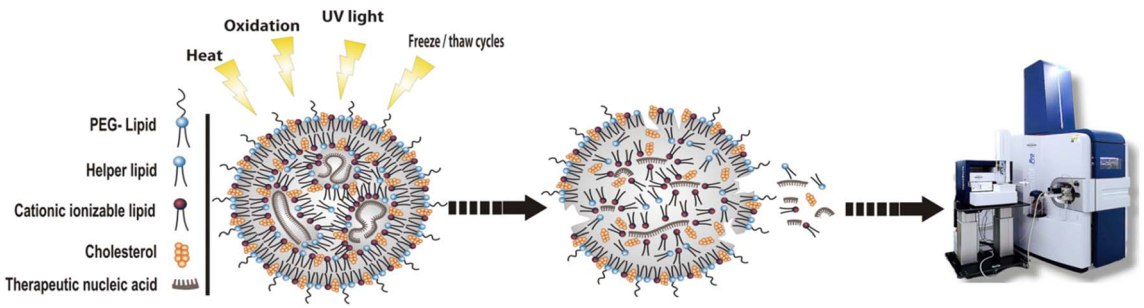

Fig. 1 Schematic overview of environmental stress-induced degradation of mRNA-LNPs and analytical workflow.

stressors affect the stability of mRNA-LNPs, thereby influencing their delivery and therapeutic potential. Secondly, to employ UHPLC techniques coupled with TIMS-TOF mass spectrometry to investigate the molecular architecture and interactions within LNPs, lastly, to identify strategies and best practices for improving the stability and durability of LNPs. These advancements hold the promise not only of enhancing the performance of current mRNA-LNP formulations but also of paving the way for the next generations of nanoparticle-based therapies.

Materials and methods

Luciferase-encoding mRNA-LNPs were formulated using three structurally distinct ionizable lipids-DLin-MC3-DMA (MC3), SM-102, and ALC-0315-to evaluate lipid-specific responses to environmental stress. Each formulation was independently prepared using the NanoAssemblr™ Spark system (Precision NanoSystems, Vancouver, Canada) following a microfluidic mixing protocol optimized for uniform particle size and encapsulation efficiency. The organic phase, containing ionizable lipid, helper phospholipid, cholesterol, and PEG-lipid dissolved in ethanol, was rapidly mixed with an aqueous phase of luciferase-encoding mRNA in citrate buffer (pH 4.0) at a fixed flow ratio to promote spontaneous self-assembly. Formulations were dialyzed against phosphate-buffered saline (PBS, pH 7.4) and characterized for particle size, polydispersity index, and encapsulation efficiency prior to stress testing.[32,63,64]

Equal aliquots of each LNP formulation were then subjected to individual stress conditions for 72 hours to simulate environmental challenges. Stress treatments included thermal stress (incubation at 28 °C), photo-oxidative stress (continuous UV exposure at 360 nm), chemical oxidation (hydrogen peroxide treatment at a final concentration of 100 mM), and mechanical stress from repeated freeze–thaw cycling (−20 °C for 12 hours followed by 22 °C for 12 hours). Control samples were maintained under standard refrigerated storage (4 °C).

Following exposure, lipids were extracted from each sample using a chloroform : methanol (2 : 1, v/v) mixture, vortexed, and centrifuged to separate phases. The organic layer was collected, evaporated under nitrogen, and reconstituted in isopropanol prior to liquid chromatography-mass spectrometry (LC-MS) analysis.

The LC-MS analyses were performed using a Bruker Elute UHPLC system coupled to a Bruker timsTOF Pro mass spectrometer. Samples were maintained at 4 °C in the autosampler, and separations were conducted at a column temperature of 55 °C with an injection volume of approximately 2 μL.

Chromatographic separation was achieved using a YMC UPLC C18 column (1.9 μm particle size, 100 Å pore size, 2.1 × 100 mm), preceded by a Triart C18 EXP guard cartridge (1.9 μm, 2.1 × 5 mm). The mobile phases consisted of mobile phase A, 60 : 40 (v/v) acetonitrile:water containing 10 mM ammonium formate and 0.1% formic acid, and mobile phase B, 90 : 10 (v/v) isopropanol:acetonitrile containing 10 mM ammonium formate and 0.1% formic acid. The flow rate was maintained at 0.400 mL min^{-1} throughout the gradient elution.

Mass spectrometric detection was performed on a Bruker timsTOF Pro equipped with a VIP-HESI source, operated in both positive and negative ionization modes. Source parameters were set as follows: nebulizer gas pressure 2.0 bar, dry gas flow 8 L min^{-1}, probe gas temperature 400 °C, and source temperature 230 °C. Capillary voltages were set to ±4500/3600 V for positive and negative modes, respectively. Ion mobility separations were conducted using trapped ion mobility spectrometry (TIMS) with a 100 ms ramp time and an ion mobility range of 0.55–1.90 V s cm^{-2} ($1/K_0$). Data were acquired over a mass range of m/z 100–1350 in full-scan MS and data-dependent MS/MS mode using DDA-PASEF acquisition.

Mass calibration was performed using sodium formate cluster ions for m/z calibration and a Bruker Tune Mix solution for ion mobility calibration. Data processing and analysis were carried out using Bruker MetaboScape (version 2025b) and Bruker DataAnalysis (version 6.2).

Results

Ribogreen for mRNA encapsulation efficiency and concentration

The mRNA concentration and encapsulation efficiency (70–90%) were determined by the Quant-IT Ribogreen assay. Tris (10 mM, pH = 7.5)/EDTA (1 mM) (TE) and Triton/TE (2% v/v Triton in TE buffer) were added in duplicates to a black microplate. Total mRNA in the LNP was diluted to ∼4 ng μL^{-1} in TE and added to each TE and TE/Triton well in a 1 : 1 volume ratio. Microplates were incubated at 37 °C for 10 min to extract LNPs with Triton. Ribogreen reagent in DMSO was diluted 1 : 100 in TE Buffer and added to each well in a 1 : 1 volume ratio. Microplates were immediately introduced into the Cytation 5 Cell Imaging Multi-Mode Reader (Biotek) to read Fluorescence (Ex485/Em528).

Size by dynamic light scattering

Nanoparticle size was 55–70 nm diameters as determined by dynamic light scattering using a Zetasizer Nano ZS. LNPs were diluted to 6.25 ng μL^{-1} total mRNA in PBS pH = 7.4 and transferred into a quartz cuvette (ZEN2112). Measurements were made using particle RI of 1.45 and absorption of 0.001 in PBS at 25 °C with viscosity of 0.888 cP and RI of 1.335. A 173° backscatter angle of detection previously equilibrated to 25 °C for 30 s in duplicates was used, each with 5 runs and 10 s run duration, without delay between measurements. Each measurement had a fixed position of 4.65 mm in the quartz cuvette with an automatic attenuation selection. Data were analyzed using a General-Purpose model with normal resolution. Diameter are reported as the number average.

In vitro transfection

HEK293 cells were seeded in white 96-well plates at a density of 12×10^3 cells per well in 100 μL EMEM medium (10% FBS) the day before transfection and incubated at 37 °C 5% CO_2. LNPs were diluted to 32 μL containing 200 ng FLuc mRNA and cells were transfected in triplicates 24 h after seeding. After a further

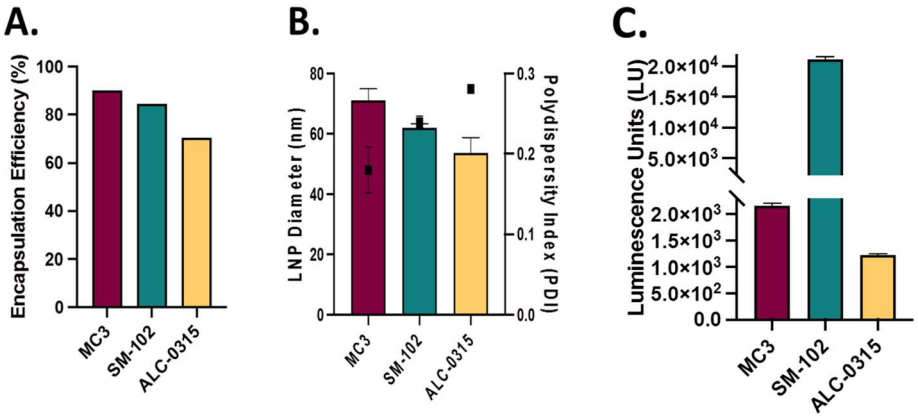

Fig. 2 Encapsulation efficiency using three ionizing lipids used in this study (panel A) and the nanoparticle diameter (panel B). Panel C demonstrates a comparison of reporter gene expression from mRNA-loaded lipid nanoparticles formulated with MC3, SM-102, and ALC-0315, measured as luminescence units (LU). A broken *y*-axis is used to accommodate the markedly higher signal observed for SM-102 relative to MC3 and ALC-0315.

24 h, 100 μL of One-Glo substrate was added directly to the wells to detect luciferase expression based on luminescence in cytation 5 luminometer plate reader. Fig. 2 displays the encapsulation efficiency and the average particle size in the tested formulations.

The encapsulation efficiency of the LNPs was assessed using the Quant-IT Ribogreen assay, yielding an efficiency of approximately 90%. The average diameter of the nanoparticles, determined by dynamic light scattering with a Zetasizer Nano ZS, was found to be between 55–70 nm. To evaluate *in vitro* expression and confirm the successful formulation of the LNPs, HEK293 cells were transfected with a 200-ng dose of the formulated nanoparticles. Our measurements confirmed the successful formulation and were consistent with the literature.

Impact of environmental stress on mRNA-LNP encapsulation efficiency

Consistent with the literature, our results indicate that mild environmental stressors, including modest heat exposure, ultraviolet irradiation, oxidative stress, and limited freeze–thaw cycling, generally do not produce immediate or measurable changes in the encapsulation efficiency (EE) of mRNA-LNPs. Encapsulation is primarily established during formulation through electrostatic complexation between ionizable lipids and mRNA, yielding a structurally robust particle that is resistant to mild post-formulation stress.[33,65,66]

Thermal stress within moderate ranges accelerates lipid oxidation and mRNA chemical degradation but does not typically disrupt particle integrity or induce mRNA release, resulting in preserved EE despite reduced biological activity.[2,34] Similarly, UV exposure predominantly induces photochemical damage to nucleobases and lipid headgroups without altering particle size or mRNA retention, leading to intact encapsulation with impaired translation efficiency.[67]

Oxidative stress, such as low-level hydrogen peroxide exposure, preferentially modifies ionizable lipids and helper lipids (*e.g.*, phosphatidylcholines), as well as mRNA bases, without causing gross membrane disruption or mRNA leakage. As a result, standard EE assays remain unchanged even though endosomal escape and functional delivery are compromised (Estabrook *et al.*, 2025).[68]

Limited freeze–thaw cycling likewise has minimal impact on EE in the presence of intact lipid packing and cryoprotective conditions, although repeated cycles may promote aggregation or functional loss prior to detectable mRNA release (Cheng *et al.*, 2025).[66] Collectively, these observations highlight a form of "silent instability", in which chemically driven degradation of lipid and mRNA components leads to loss of potency without detectable changes in encapsulation efficiency, particle size, or polydispersity. This underscores the limitation of EE as a standalone stability metric and emphasizes the need for chemically sensitive analytical methods to assess mRNA-LNP integrity and performance.

LC-MS analysis

The LC-MS analysis revealed that MC3, SM-102, and ALC-0315 lipids showed significant degradation when exposed to UV light and hydrogen peroxide. While heating and freeze/thaw cycles had minimal impact on the ionizable lipids in mRNA-LNPs, UV light and oxidative conditions were particularly detrimental. The degradation products resulting from UV exposure and oxidation were strikingly similar, suggesting a free radical mechanism initiated by atmospheric oxygen. Our findings, in comparison to other stability studies, emphasize the mechanistic synthesis aligning with reports that light exposure reduces expression without altering size, polydispersity index (PDI), and mRNA retention (fluorescent light 1000–6000 l× for 20 h). Emphasizing that more chemical damage occurs, causing the results shown in other studies, rather than visible physical changes. Using the UHPLC-TIMS-TOF, we were able to identify and give an explanation for the chemical damage at the position, with confirmation of the specific headgroups of ionizable lipids such as MC3 (+1 O). Concluding that these results fit well with QC tests, the single-

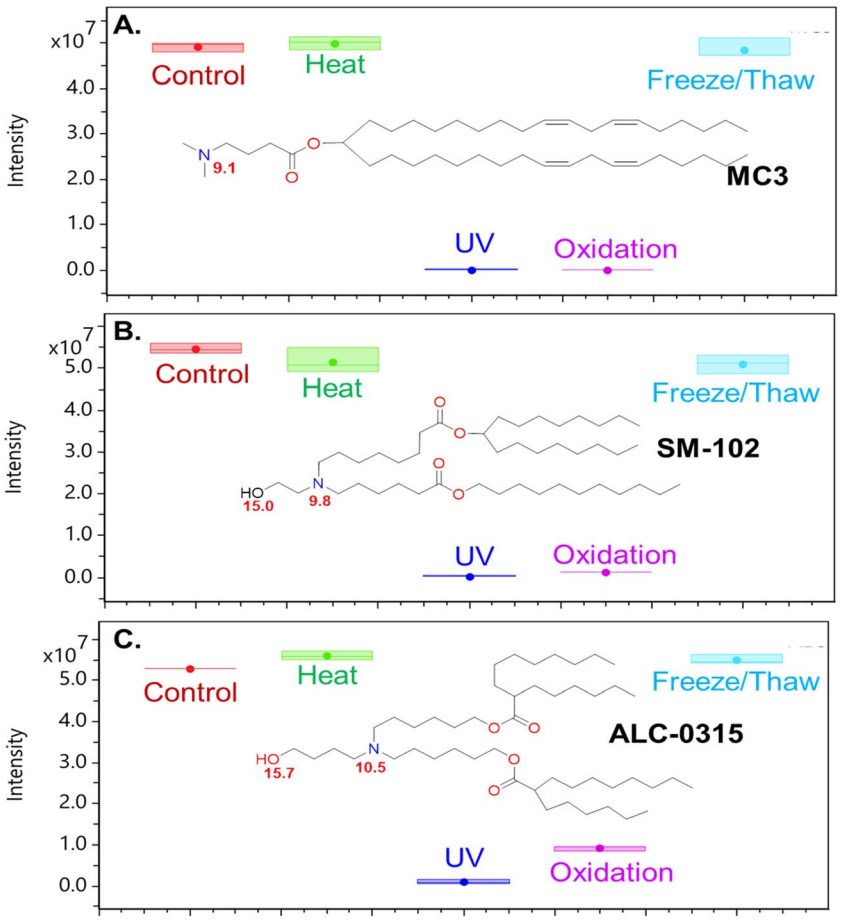

Fig. 3 A box plot demonstrating the ionizing lipid ion intensities of (A) MC3, (B) SM-102 and (C) ALC-0315 measured by LC-MS in control and after stress-induced degradation.

quadrupole RPLC-MS method, which is known to detect early oxidation markers (such as aldehydes after DNPH derivatization). Fig. 3 demostrates Box plots showing the ion intensities of the ionizable lipids (A) MC3, (B) SM-102, and (C) ALC-0315 measured by LC-MS under control conditions and following stress-induced degradation.

Specifically, MC3 was highly susceptible to both oxidative conditions and UV light, with the primary oxidation product being MC3 + one oxygen. The fragmentation pattern indicated that the additional oxygen was inserted between the tertiary nitrogen and the ester group, leaving the lipid's tail end intact. A significant degradation marker for MC3 was identified at m/z = 609.6039, indicating cleavage of the ionizable tertiary nitrogen head. Fig. 4 demonstrate the LCMS analysis of LNP mixture containing MC3: (I) control sample and (II) UV-stressed sample. (A) Base peak chromatogram of the mixture, and (B) retention time – ion mobility heat map.

Hydrogen peroxide caused oxidation of DSPC, specifically between the quaternary head and the phosphate group, with a degradation marker found at m/z = 593.5978. Fig. 5 displays the MS/MS spectra to confirm oxidation of DSPC.

For SM-102, oxidizing conditions led to the formation of a carboxylate adduct, while UV light resulted in the addition of a hydroxyl group on a carbon near the hydroxyl terminus, likely *via* a free radical mechanism. This was corroborated by the fragmentation pattern of m/z = 726.6613. Three levels of oxidation were observed for SM-102: SM102 + one oxygen (carboxylate adduct), SM102 + two oxygens, and SM102 + three oxygens. Fig. 6 shows an overlay of the MS/MS spectra of SM102 and the oxidation by product thereof.

The ALC-0315 lipid demonstrated multiple levels of oxidation (ALC + one oxygen and ALC-0315 + two oxygens) and extensive alpha cleavage along with numerous C–C cleavages near the hydroxyl terminus. These findings underline the vulnerability of these ionizable lipids to oxidative stress and UV light, emphasizing the importance of considering these factors in the formulation and storage of mRNA-LNPs.

Discussion

This study systematically characterizes how the clinically relevant ionizable lipids DLin-MC3-DMA (MC3), SM-102, and ALC-0315 in mRNA-LNPs undergo chemical degradation under realistic environmental stress conditions, and demonstrates why conventional stability metrics can fail to detect this "silent" degradation. Luciferase-encoding mRNA-LNPs were formulated

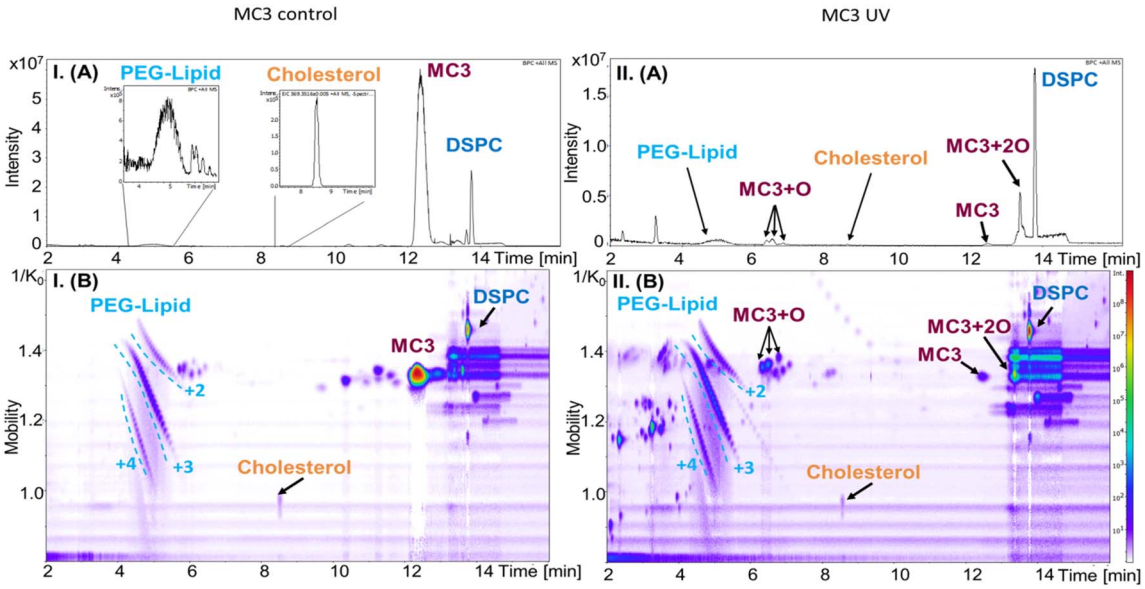

Fig. 4 Analysis of LNP mixture containing MC3: (I) control and (II) under UV stress. (A) Base peak chromatogram of the mixture, and (B) heat map of retention time-ion mobility.

by microfluidic mixing and exposed for 72 hours to mild heat, UV irradiation, hydrogen peroxide-driven oxidation, or repeated freeze–thaw cycles, then interrogated using UHPLC-TIMS-TOF MS to resolve intact lipids and degradation products with high structural specificity. While particle size, polydispersity, encapsulation efficiency, and *in vitro* expression initially appeared acceptable, TIMS-TOF analysis revealed that UV and oxidative stress, not modest heating or freeze–thaw, induced extensive, lipid-dependent headgroup oxidation, ester hydrolysis, and bond cleavage in MC3, SM-102, ALC-0315, and DSPC,

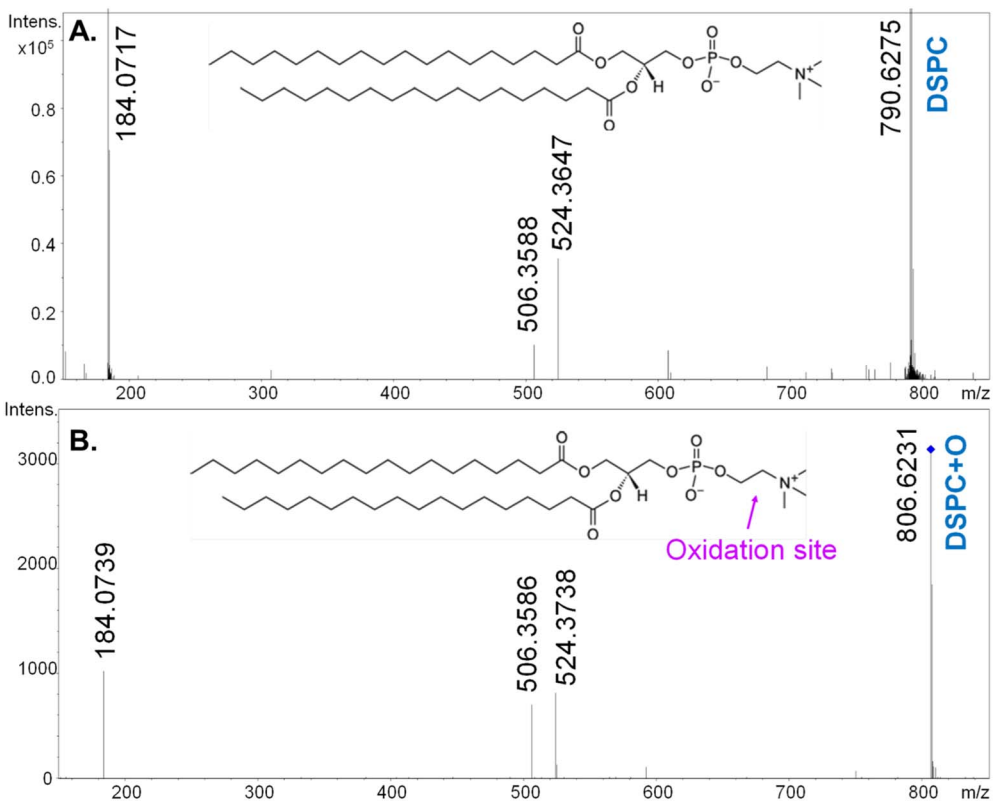

Fig. 5 The MS/MS spectra of (A) DSPC and (B) oxidized DSPC after H_2O_2 treatment.

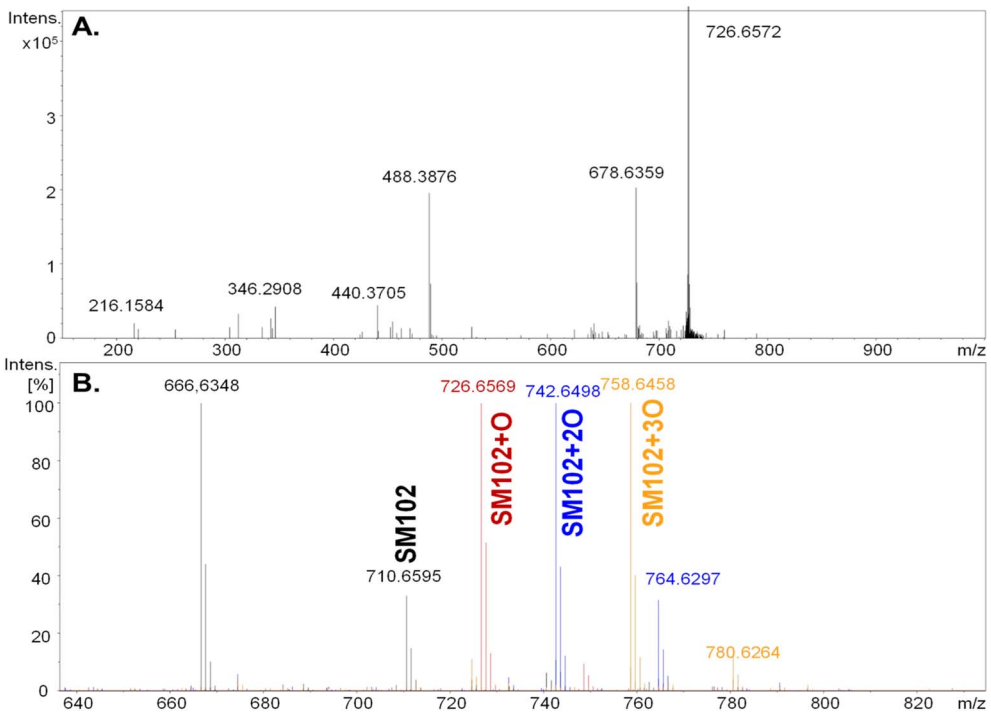

Fig. 6 The MS/MS spectra of (A) oxidized SM102 at $m/z = 726$ and (B) overlaid MS spectra of SM102 and three levels of oxidation forms.

at sites critical for endosomal escape and functional delivery. By mapping these discrete oxidative pathways and aligning them with prior functional observations in the literature, the work establishes ionizable lipid oxidation as a primary mechanistic driver of hidden potency loss and positions UHPLC-TIMS-TOF MS as a powerful stability-indicating platform to guide formulation design, handling practices, and regulatory-quality control for mRNA LNP therapeutics.

A recent study by Kamiya *et al.*[33] aimed to assess the impact of various environmental stressors of LNP stability. The study focused on evaluating the performance of mRNA-LNPs formulated by DLin-MC3-DMA (MC3) in a 50 : 10 : 38.5 : 1.5 ratio with DSPC, cholesterol, and DMG-PEG2000. Different stressors were used, including temperature, light, vibration, syringe handling, and the presence or absence of a cryoprotectant (sucrose). Stability was measured by comparing particle size, mRNA retention, and luciferase protein expression, along with confirming mRNA integrity using agarose gel electrophoresis. The results showed that the LNPs went through morphological changes due to the absence of sucrose, which caused clumping and reduced protein expression, highlighting that sucrose plays a major functional role in preventing aggregation and maintaining protein expression activity. The data also demonstrated that environmental stressors such as strong shaking or vortexing for 5 minutes damaged the nanoparticles, in contrast to gentle tapping or drawing the vaccine into syringes multiple times, which did not cause harm. The most notable finding was that exposure to visible light reduced protein expression while particle size, mRNA retention, and band length remained intact, leading Kamiya's team to suggest that this hidden effect was likely caused by oxidation of the lipids or mRNA. However, they were unable to directly identify or quantify the chemical damage incurred by the ionizable lipids.

Our UHPLC-TIMS-TOF analysis helped explain why Kamiya's hidden effect was likely caused by oxidation and degradation of the lipids, not the mRNA. In our study, we observed that MC3 gained an oxygen atom (MC3 + 1O), and similar oxidation patterns were found in SM-102, ALC-0315, and even the helper lipid DSPC, supporting that UV light and oxidative stress lead to chemical damage of the ionizable lipids themselves. Our data emphasize that these reactions occurred at the lipid headgroups, where oxidation broke key bonds that help the nanoparticles release mRNA inside cells. It is important to note that these molecular changes do not always alter particle size, which explains why Kamiya's testing did not show changes in size even though function was failing. Altogether, both studies have shown a similar pattern, demonstrating that light and oxygen exposure quietly damage LNPs, while other factors such as controlled temperature, freezing with cryoprotectant, and gentle handling help maintain stability.

Another interesting study that has caught our attention was by Birdsall *et al.*[69] Birdsall's team developed a QC-friendly RPLC-MS (single-quadrupole) method to quantify and detect low-level, impurities that could be found in LNP-formulated products and raw materials, focusing on both ALC-0315 and SM-102. Their MS configuration achieved a 100- to 1000-fold improvement in sensitivity and dynamic range, allowing routine detection of reactive degradation products, including N-oxides, imines, and aldehydes, that form under oxidative or pH stress and even during short-term room-temperature storage, outperforming conventional detectors such as Evaporative Light-Scattering Detection (ELSD) and Charged Aerosol Detection

(CAD). The results were obtained using 2,4-dinitrophenylhydrazine derivatization (DNPH derivatization), and they were able to quantify aldehydes (*e.g.*, 6-oxohexyl 2-hexyldecanoate) in several batches of ALC-0315. Results showed that aldehydes were carried over into both empty and mRNA-loaded LNPs. These aldehyde levels were then linked to several mRNA-adduct peaks observed over 7 days, proving that reactive lipid products can weaken activity even when optical tests fail to detect them.

This study pairs with our work because our UHPLC-TIMS-TOF mapped the exact oxidized lipid species responsible for those functional losses (MC3 + 1O, staged SM-102 (+1–3O), and ALC-0315 (+1–2O)). We also detected and pinpointed the exact oxidation sites on the headgroup, emphasizing the ROS-driven chemistry that disrupts delivery efficiency without necessarily shifting DLS metrics. Combining both studies offers a complementary practical workflow: Birdsall's method provides a quick way to screen for early oxidation markers such as N-oxides and aldehydes in raw lipids and finished LNPs, while our TIMS-TOF analysis confirms and identifies which lipids were chemically altered through structural hallmarks. Together, these approaches strengthen quality control by ensuring minimal light and oxygen exposure and by monitoring aldehyde formation and variability in lipid materials of different paths.

Along with reviewing the literature, a recent study by Schoenmaker *et al.*[23] systematically investigated the stability of Pfizer- and Moderna-type mRNA-LNPs under real-world storage and handling conditions. The Schoenmaker team documented several changes in the samples' particle size, PDI, and encapsulation when samples were stored between −80 °C and 25 °C, along with possible repeated freeze–thaw cycling. Physical degradation and mRNA leakage were documented to occur rapidly above −20 °C, with size and PDI increases signaling loss of integrity. The study attributed this mainly to mRNA hydrolysis but did not perform any mapping of either lipidomics or oxidation to explain the mechanisms driving this loss, leaving a huge gap in mechanistic literature. Our UHPLC-TIMS-TOF data clarify this gap by explaining that the reason was headgroup oxidation and ester hydrolysis in MC3, SM-102, and ALC-0315 that occur even under mild temperature shifts before visible aggregation was documented by the Schoenmaker team.

Similar to Schoenmaker *et al.*,[23] another study by Muramatsu *et al.*[65] investigated the long-term stability of nucleoside-modified mRNA-LNPs, built with the same lipid architecture used in most clinical mRNA vaccines. The formulation contained a typical ionizable lipid, (6*Z*,16*Z*)-12-((*Z*)-dec-4-en-1-yl) docosa-6,16-dien-11-yl 5-(dimethylamino)pentanoate, along with DSPC, cholesterol, and PEG-lipid in a 50 : 10 : 38.5 : 1.5 molar ratio. Muramatsu's team focused on exposing both wet and lyophilized formulations to multiple storage stressors, including a range of temperatures (−80 °C, −20 °C, 4 °C, 25 °C, and 42 °C) for up to 24 weeks, followed by reconstitution and testing. Measurements included dynamic light scattering (DLS) for particle size and PDI, RiboGreen assays for mRNA encapsulation, capillary electrophoresis for mRNA integrity, and UHPLC-CAD for individual lipid quantification. Results illustrated that both physical parameters and encapsulation remained stable, and luciferase and HA mRNA vaccines preserved their *in vivo* translation and immunogenicity under mild conditions (around 4 °C and below). In contrast, higher temperature exposure (42 °C) caused significant mRNA degradation (∼70% integrity loss) and functional decline, despite lipid ratios and particle size remaining constant. Muramatsu's team concluded that an unknown chemical reaction rather than physical instability had occurred but were uncertain of the exact mechanistic cause.

Our UHPLC-TIMS-TOF results provide the missing piece needed to explain this mechanistic gap and why Muramatsu's team could not directly track ionizable-lipid chemistry. Their UHPLC method confirmed lipid composition but lacked oxidation-sensitive detection, leaving them to infer degradation only from the loss of biological activity. By contrast, our data reveal that there is more to the story: under UV and oxidative stress, oxidation and headgroup cleavage occur within the ionizable lipid core (MC3 + 1O and similar patterns in SM-102 and ALC-0315). These molecular changes disrupt the tertiary-amine charge balance required for endosomal fusion, explaining the sharp drop in protein expression at 42 °C without shifting DLS results. In summary, our results chemically map the backbone of what Muramatsu's team observed biologically, showing that heat and oxygen trigger early oxidation at the ionizable-lipid headgroups before visible aggregation occurs, defining a clear chemical pathway for high-temperature LNP degradation, while Muramatsu's results highlight when potency is lost.

Conclusion

This work establishes a direct and mechanistically grounded link between environmental stressors and the chemical degradation of ionizable lipids at the core of mRNA LNP stability. By systematically interrogating MC3, SM-102, and ALC-0315 under controlled UV, oxidative, thermal, and freeze–thaw conditions, and resolving their degradation fingerprints using UHPLC-TIMS-TOF MS, we demonstrate that the most consequential vulnerabilities of mRNA-LNPs arise not from gross physical destabilization, but from subtle, site-specific oxidative transformations of ionizable and helper lipids. UV irradiation and hydrogen peroxide exposure induced pronounced oxidation, headgroup cleavage, and ester hydrolysis in all three ionizable lipids and DSPC, while mild heat and repeated freeze–thaw cycling had comparatively limited impact on their chemical integrity. Importantly, these molecular insults occurred in regimes where conventional metrics, particle size, polydispersity, and encapsulation efficiency, remained largely unchanged, revealing a "silent degradation" window in which LNPs may retain acceptable physicochemical profiles yet suffer functional decline.

Our findings reconcile and extend prior stability studies that observed loss of expression or potency in the absence of overt changes in bulk properties, by pinpointing ionizable lipid headgroup oxidation and reactive degradation products as primary drivers of performance failure. In doing so, this work underscores that robust evaluation of mRNA-LNP quality

cannot rely solely on DLS, RiboGreen, or compositional assays, but must incorporate chemically sensitive, stability-indicating methods capable of detecting low-abundance oxidative species and bond-specific damage. The UHPLC-TIMS-TOF platform presented here offers such resolution, providing structural assignment, isomer separation, and mechanistic insight into degradation pathways that are directly actionable for formulation design and quality control.

Collectively, these results have significant implications for the development, handling, and regulation of mRNA-based therapeutics. They highlight the critical need to minimize light and oxidative exposure throughout manufacturing, storage, and distribution, particularly as mRNA vaccines and therapies expand into global settings with variable infrastructure. They also provide a rational framework for engineering next-generation ionizable lipids with enhanced resistance to oxidation and for integrating orthogonal analytical workflows—combining high-resolution MS with QC-friendly assays, to monitor and mitigate deleterious chemical changes over product lifetime. By chemically defining the failure modes of current ionizable lipids, this study advances both the scientific understanding and practical control of mRNA LNP stability, paving the way toward safer, more durable, and more reliable nucleic acid nanomedicines.

Author contributions

Study Design: Michael Girgis, Erica Forsberg, and Mikell Paige; methodology and sample preparation: Suman Alishetty, Manuel Carrasco, Dillon O'Neill, Nabilah Baby, and Gregory Petruncio; data acquisition: Mathew Albano, Xuejun Peng, Beixi Wang, and Erica Forsberg; data analysis and visualization: Michael Girgis, Amir Saed, Beixi Wang, Amany Saleh, and Mikell Paige; writing/editing the original manuscript: Michael Girgis, Caroline Hoemann, Erica Forsberg, Mohammad Rahil. Amany Saleh, Paul Russo, and Mikell Paige; supervision: Caroline Hoemann, Erica Forsberg, and Mikell Paige.

Conflicts of interest

The authors declare no conflict of interest.

Data availability

All data supporting the findings of this study are provided in the article and its supplementary information (SI). Raw UHPLC-TIMS-TOF MS raw data files are available at jPOST repository (accession number PXD075449) at https://repository.jpostdb.org/entry/JPST004453. Supplementary information is available. See DOI: https://doi.org/10.1039/d5ra08835f.

Acknowledgements

This work was supported by the National Science Foundation (Award: 2413335), the Center for Applied Proteomics and Molecular Medicine, and the Center for Molecular Engineering at George Mason University.

References

1 R. Tenchov, R. Bird, A. E. Curtze and Q. Zhou, Lipid Nanoparticles horizontal line From Liposomes to mRNA Vaccine Delivery, a Landscape of Research Diversity and Advancement, *ACS Nano*, 2021, **15**(11), 16982–17015.
2 X. Hou, T. Zaks, R. Langer and Y. Dong, Lipid nanoparticles for mRNA delivery, *Nat. Rev. Mater.*, 2021, **6**(12), 1078–1094.
3 L. Yang, L. Gong, P. Wang, *et al.*, Recent Advances in Lipid Nanoparticles for Delivery of mRNA, *Pharmaceutics*, 2022, **14**, 2682.
4 Y. Zong, Y. Lin, T. Wei and Q. Cheng, Lipid Nanoparticle (LNP) Enables mRNA Delivery for Cancer Therapy, *Adv. Mater.*, 2023, **35**(51), e2303261.
5 M. Qiu, Y. Li, H. Bloomer and Q. Xu, Developing Biodegradable Lipid Nanoparticles for Intracellular mRNA Delivery and Genome Editing, *Acc. Chem. Res.*, 2021, **54**(21), 4001–4011.
6 A. M. Reichmuth, M. A. Oberli, A. Jaklenec, R. Langer and D. Blankschtein, mRNA vaccine delivery using lipid nanoparticles, *Ther. Delivery*, 2016, **7**(5), 319–334.
7 X. Wang, S. Liu, Y. Sun, *et al.*, Preparation of selective organ-targeting (SORT) lipid nanoparticles (LNPs) using multiple technical methods for tissue-specific mRNA delivery, *Nat. Protoc.*, 2023, **18**(1), 265–291.
8 R. S. Riley, M. V. Kashyap, M. M. Billingsley, *et al.*, Ionizable lipid nanoparticles for in utero mRNA delivery, *Sci. Adv.*, 2021, **7**, aba1028.
9 M. P. Lokugamage, D. Vanover, J. Beyersdorf, *et al.*, Optimization of lipid nanoparticles for the delivery of nebulized therapeutic mRNA to the lungs, *Nat. Biomed. Eng.*, 2021, **5**(9), 1059–1068.
10 K. Swetha, N. G. Kotla, L. Tunki, *et al.*, Recent Advances in the Lipid Nanoparticle-Mediated Delivery of mRNA Vaccines, *Vaccines*, 2023, **11**, 0658.
11 B. Wilson and K. M. Geetha, Lipid nanoparticles in the development of mRNA vaccines for COVID-19, *J. Drug Delivery Sci. Technol.*, 2022, **74**, 103553.
12 M. M. Billingsley, N. Singh, P. Ravikumar, R. Zhang, C. H. June and M. J. Mitchell, Ionizable Lipid Nanoparticle-Mediated mRNA Delivery for Human CAR T Cell Engineering, *Nano Lett.*, 2020, **20**(3), 1578–1589.
13 L. Miao, Y. Zhang and L. Huang, mRNA vaccine for cancer immunotherapy, *Mol. Cancer*, 2021, **20**(1), 41.
14 Y. L. Vishweshwaraiah and N. V. Dokholyan, mRNA vaccines for cancer immunotherapy, *Front. Immunol.*, 2022, **13**, 1029069.
15 J. Q. Liu, C. Zhang, X. Zhang, *et al.*, Intratumoral delivery of IL-12 and IL-27 mRNA using lipid nanoparticles for cancer immunotherapy, *J. Controlled Release*, 2022, **345**, 306–313.
16 E. Kon, N. Ad-El, I. Hazan-Halevy, L. Stotsky-Oterin and D. Peer, Targeting cancer with mRNA-lipid nanoparticles: key considerations and future prospects, *Nat. Rev. Clin. Oncol.*, 2023, **20**(11), 739–754.

17 C. Wang, Y. Zhang and Y. Dong, Lipid Nanoparticle-mRNA Formulations for Therapeutic Applications, *Acc. Chem. Res.*, 2021, **54**(23), 4283–4293.
18 D. Witzigmann, J. A. Kulkarni, J. Leung, S. Chen, P. R. Cullis and R. van der Meel, Lipid nanoparticle technology for therapeutic gene regulation in the liver, *Adv. Drug Delivery Rev.*, 2020, **159**, 344–363.
19 D. An, J. L. Schneller, A. Frassetto, *et al.*, Systemic Messenger RNA Therapy as a Treatment for Methylmalonic Acidemia, *Cell Rep.*, 2017, **21**(12), 3548–3558.
20 H. Attarwala, M. Lumley, M. Liang, V. Ivaturi and J. Senn, Translational Pharmacokinetic/Pharmacodynamic Model for mRNA-3927, an Investigational Therapeutic for the Treatment of Propionic Acidemia, *Nucleic Acid Ther.*, 2023, **33**(2), 141–147.
21 M. Jeong, Y. Lee, J. Park, H. Jung and H. Lee, Lipid nanoparticles (LNPs) for *in vivo* RNA delivery and their breakthrough technology for future applications, *Adv. Drug Delivery Rev.*, 2023, **200**, 114990.
22 N. Al Fayez, M. S. Nassar, A. A. Alshehri, *et al.*, Recent Advancement in mRNA Vaccine Development and Applications, *Pharmaceutics*, 2023, **15**, 1972.
23 L. Schoenmaker, D. Witzigmann, J. A. Kulkarni, *et al.*, mRNA-lipid nanoparticle COVID-19 vaccines: Structure and stability, *Int. J. Pharm.*, 2021, **601**, 120586.
24 B. E. Oude, E. Ornskov, C. Schoneich, *et al.*, The Storage and In-Use Stability of mRNA Vaccines and Therapeutics: Not A Cold Case, *J. Pharm. Sci.*, 2023, **112**(2), 386–403.
25 S. Ramachandran, S. R. Satapathy and T. Dutta, Delivery Strategies for mRNA Vaccines, *Pharm. Med.*, 2022, **36**(1), 11–20.
26 B. Kim, R. R. Hosn, T. Remba, *et al.*, Optimization of storage conditions for lipid nanoparticle-formulated self-replicating RNA vaccines, *J. Controlled Release*, 2023, **353**, 241–253.
27 A. De and Y. T. Ko, Why mRNA-ionizable LNPs formulations are so short-lived: causes and way-out, *Expert Opin. Drug Delivery*, 2023, **20**(2), 175–187.
28 M. Kloczewiak, J. M. Banks, L. Jin and M. L. Brader, A Biopharmaceutical Perspective on Higher-Order Structure and Thermal Stability of mRNA Vaccines, *Mol. Pharmaceutics*, 2022, **19**(7), 2022–2031.
29 A. Thaller, L. Schmauder, W. Friess, *et al.*, SV-AUC as a stability-indicating method for the characterization of mRNA-LNPs, *Eur. J. Pharm. Biopharm.*, 2023, **182**, 152–156.
30 W. Yihunie, G. Nibret and Y. Aschale, Recent Advances in Messenger Ribonucleic Acid (mRNA) Vaccines and Their Delivery Systems: A Review, *Clin. Pharmacol.*, 2023, **15**, 77–98.
31 Y. Hirai, R. Saeki, F. Song, *et al.*, Charge-reversible lipid derivative: A novel type of pH-responsive lipid for nanoparticle-mediated siRNA delivery, *Int. J. Pharm.*, 2020, **585**, 119479.
32 L. Zhang, K. R. More, A. Ojha, *et al.*, Effect of mRNA-LNP components of two globally-marketed COVID-19 vaccines on efficacy and stability, *npj Vaccines*, 2023, **8**(1), 156.
33 M. Kamiya, M. Matsumoto, K. Yamashita, *et al.*, Stability Study of mRNA-Lipid Nanoparticles Exposed to Various Conditions Based on the Evaluation between Physicochemical Properties and Their Relation with Protein Expression Ability, *Pharmaceutics*, 2022, **14**, 2357.
34 F. Cheng, Y. Wang, Y. Bai, *et al.*, Research Advances on the Stability of mRNA Vaccines, *Viruses*, 2023, **15**, 0668.
35 S. H. Kiaie, N. Majidi Zolbanin, A. Ahmadi, *et al.*, Recent advances in mRNA-LNP therapeutics: immunological and pharmacological aspects, *J. Nanobiotechnol.*, 2022, **20**(1), 276.
36 B. Z. Igyarto and Z. Qin, The mRNA-LNP vaccines – the good, the bad and the ugly?, *Front. Immunol.*, 2024, **15**, 1336906.
37 K. Broudic, A. Amberg, M. Schaefer, H. P. Spirkl, M. C. Bernard and P. Desert, Nonclinical safety evaluation of a novel ionizable lipid for mRNA delivery, *Toxicol. Appl. Pharmacol.*, 2022, **451**, 116143.
38 P. Berraondo, P. G. V. Martini, M. A. Avila and A. Fontanellas, Messenger RNA therapy for rare genetic metabolic diseases, *Gut*, 2019, **68**(7), 1323–1330.
39 Y. S. Wang, M. Kumari, G. H. Chen, *et al.*, mRNA-based vaccines and therapeutics: an in-depth survey of current and upcoming clinical applications, *J. Biomed. Sci.*, 2023, **30**(1), 84.
40 M. Chehelgerdi and M. Chehelgerdi, The use of RNA-based treatments in the field of cancer immunotherapy, *Mol. Cancer*, 2023, **22**(1), 106.
41 L. Wu, X. Li, X. Qian, S. Wang, J. Liu and J. Yan, Lipid Nanoparticle (LNP) Delivery Carrier-Assisted Targeted Controlled Release mRNA Vaccines in Tumor Immunity, *Vaccines*, 2024, **12**, 0186.
42 J. Han, J. Lim, C. J. Wang, *et al.*, Lipid nanoparticle-based mRNA delivery systems for cancer immunotherapy, *Nano Convergence*, 2023, **10**(1), 36.
43 V. P. Zhdanov, Kinetics of lipid-nanoparticle-mediated intracellular mRNA delivery and function, *Phys. Rev. E*, 2017, **96**(4–1), 042406.
44 N. Aliakbarinodehi, A. Gallud, M. Mapar, *et al.*, Interaction Kinetics of Individual mRNA-Containing Lipid Nanoparticles with an Endosomal Membrane Mimic: Dependence on pH, Protein Corona Formation, and Lipoprotein Depletion, *ACS Nano*, 2022, **16**(12), 20163–20173.
45 G. Tilstra, J. Couture-Senecal, Y. M. A. Lau, *et al.*, Iterative Design of Ionizable Lipids for Intramuscular mRNA Delivery, *J. Am. Chem. Soc.*, 2023, **145**(4), 2294–2304.
46 J. Chen, Y. Xu, M. Zhou, *et al.*, Combinatorial design of ionizable lipid nanoparticles for muscle-selective mRNA delivery with minimized off-target effects, *Proc. Natl. Acad. Sci. U. S. A.*, 2023, **120**(50), e2309472120.
47 M. J. Carrasco, S. Alishetty, M. G. Alameh, *et al.*, Ionization and structural properties of mRNA lipid nanoparticles influence expression in intramuscular and intravascular administration, *Commun. Biol.*, 2021, **4**(1), 956.
48 H. Huo, X. Cheng, J. Xu, J. Lin, N. Chen and X. Lu, A fluorinated ionizable lipid improves the mRNA delivery efficiency of lipid nanoparticles, *J. Mater. Chem. B*, 2023, **11**(19), 4171–4180.

49 S. H. Sakers, G. Fiduccia, K. E. Byrne, B. P. K. Reddy, J. E. Dahlman and M. R. Prausnitz, The effect of mRNA-lipid nanoparticle composition on stability during microneedle patch manufacturing, *Eur. J. Pharm. Biopharm.*, 2025, **215**, 114819.
50 W. Liu, M. Zhang, H. Lv and C. Yang, Formulation-Driven Optimization of PEG-Lipid Content in Lipid Nanoparticles for Enhanced mRNA Delivery *In Vitro* and *In Vivo*, *Pharmaceutics*, 2025, **17**, 0950.
51 C. R. Thorn, J. C. Hickey, Y. C. Chi, *et al.*, Alternative Structural Lipids Impact mRNA-Lipid Nanoparticle Morphology, Stability, and Activity, *Mol. Pharmaceutics*, 2026, **23**(1), 209–223.
52 M. M. Mader, R. Rotermund, R. Lefering, *et al.*, The faster the better? Time to first CT scan after admission in moderate-to-severe traumatic brain injury and its association with mortality, *Neurosurg. Rev.*, 2021, **44**(5), 2697–2706.
53 K. K. Peiry, Triggers for treaty negotiations: could lessons from environmental protection inform a prospective pandemic treaty?, *Bmj*, 2021, **375**, e068903.
54 A. Aburizik, M. Brindle, E. Johnson, A. Provencio, M. Kivlighan and B. LeBeau, Black women's distress matters: Examining gendered racial disparities in psycho-oncology referral rates, *Psycho-Oncology*, 2023, **32**(6), 933–941.
55 Y. Yan, J. Yang, Z. Zhu, B. Jin, R. Zhu and S. Li, Enhancing performance evaluation and microbial community analysis of the biofilter for toluene removal by adding polyethylene glycol-600 into the nutrient solution, *Bioresour. Technol.*, 2021, **330**, 124954.
56 M. Garg, D. Dhariwal and C. Newlands, Providing national level teaching to OMFS specialty trainees in a virtual classroom setting using learning theories of education, *Br. J. Oral Maxillofac. Surg.*, 2022, **60**(1), 3–10.
57 W. I. Ibraheem, A. A. Hakami, A. A. Shafei, *et al.*, Evaluating Soft Tissue Healing after Implant Placement Using Two Different Mouthwashes (Myrrh and Chlorhexidine Gluconate): A Randomized Control Trial, *Medicina*, 2022, **58**, 1351.
58 S. Y. Lin, S. C. Tang, C. H. Kuo, *et al.*, Factors affecting serum concentration of dabigatran in Asian patients with non-valvular atrial fibrillation, *J. Formosan Med. Assoc.*, 2019, **118**(7), 1154–1160.
59 D. Wainwright, M. Harris and E. Wainwright, Correction to: How does 'banter' influence trainee doctors' choice of career? A qualitative study, *BMC Med. Educ.*, 2019, **19**(1), 313.
60 N. Ashraf, S. Basu, K. Narula, *et al.*, Integrative network analyses of wilt transcriptome in chickpea reveal genotype dependent regulatory hubs in immunity and susceptibility, *Sci. Rep.*, 2018, **8**(1), 6528.
61 X. Cheng, L. Huang, L. Zhang, Q. Ai, L. Chen and Y. Chen, Multi-Chlorine-Substituted Self-Assembled Molecules As Anode Interlayers: Tuning Surface Properties and Humidity Stability for Organic Photovoltaics, *ACS Appl. Mater. Interfaces*, 2017, **9**(10), 9204–9212.
62 R. Ranjan, A. Sinha, N. Asif, S. Ifthekar, A. Kumar and S. Chand, Management of Neglected Lateral Condyle Fracture of Humerus: A Comparison between Two Modalities of Fixation, *Indian J. Orthop.*, 2018, **52**(4), 423–429.
63 N. Buawangpong, K. Pinyopornpanish, S. Pliannuom, *et al.*, Designing Telemedicine for Older Adults With Multimorbidity: Content Analysis Study, *JMIR Aging*, 2024, **7**, e52031.
64 W. Zhang, A. Pfeifle, C. Lansdell, *et al.*, The Expression Kinetics and Immunogenicity of Lipid Nanoparticles Delivering Plasmid DNA and mRNA in Mice, *Vaccines*, 2023, **11**, 1580.
65 H. Muramatsu, K. Lam, C. Bajusz, *et al.*, Lyophilization provides long-term stability for a lipid nanoparticle-formulated, nucleoside-modified mRNA vaccine, *Mol. Ther.*, 2022, **30**(5), 1941–1951.
66 X. Cheng, X. Zheng, K. Tao, *et al.*, Freezing induced incorporation of betaine in lipid nanoparticles enhances mRNA delivery, *Nat. Commun.*, 2025, **16**(1), 4700.
67 A. Heidrich, M. Hofer and V. Bohm, Protective Effects of Natural Lipophilic Antioxidants on UV-Induced Lipid Oxidation in Liposomes and Their Enhancement, *Antioxidants*, 2025, **14**, 1450.
68 D. A. Estabrook, L. Huang, O. R. Lucchese, *et al.*, Buffer optimization of siRNA-lipid nanoparticles mitigates lipid oxidation and RNA-lipid adduct formation, *Nat. Commun.*, 2025, **16**(1), 8380.
69 R. E. Birdsall, D. Han, K. DeLaney, *et al.*, Monitoring stability indicating impurities and aldehyde content in lipid nanoparticle raw material and formulated drugs, *J. Chromatogr. B:Anal. Technol. Biomed. Life Sci.*, 2024, **1234**, 124005.